

# Effect of Solvent Quality toward the Association of Succinimide Pendants of a Modified Ethylene–Propylene Copolymer in Mixtures of Toluene and Hexane

Mingzhen Zhang and Jean Duhamel\*

*Institute for Polymer Research, Department of Chemistry, University of Waterloo, Waterloo, Ontario N2L 3G1, Canada*

*Received March 15, 2005*

**ABSTRACT:** A maleated ethylene–propylene random copolymer (EP) was reacted with 1-pyrenemethylamine to yield a pyrene labeled EP, and the photophysical properties of the pyrene label were used to determine the level of aggregation between the resulting succinimide groups as a function of the composition of hexane/toluene mixtures. In hexane, the polar succinimides bearing the pyrenyl pendants form aggregates whose presence can be inferred from fluorescence and UV–vis absorption measurements. Addition of toluene is found to melt the pyrene aggregates. The aggregation induced by the polar succinimide groups was shown to occur intramolecularly at polymer concentrations of 0.1 g/L by fluorescence resonance energy transfer. The level of pyrene aggregation ( $f_{\text{agg}}$ ) was determined quantitatively and could be followed as a function of the volume fraction of hexane in a series of toluene/hexane mixtures. Upon addition of toluene, the parameter  $f_{\text{agg}}$  decreased rapidly to a finite value different from 0.0 due to the inherent clustering of succinic anhydride groups occurring during the maleation of EP. This lowest  $f_{\text{agg}}$  value was reached for a mixture containing 60 vol % of hexane. The ability of toluene at melting the pyrene aggregates was shown to have a profound effect on the rheological properties of the polymer solutions.

## Introduction

Although maleated polyolefins have been commercially produced and studied for over 50 years, a detailed knowledge of their properties is still lacking since a 2003 review refers to “the production and application of maleic anhydride grafted polyolefins (as being) currently still more resembling of alchemy than technology”.<sup>1</sup> Certainly one of the main complications in the study of maleated polyolefins has to do with the low level of grafting usually required for EP–MAHs which hinders the characterization of the succinic anhydride moieties. Most studies on EP–MAHs deal with levels of MAH grafting lower than 2 wt %. In the case of maleated polyethylene or polypropylene which can be taken as the two extremes of compositions for EP copolymers, such levels of grafting represent one succinic anhydride (SAH) unit per 173 or 116 monomers, respectively. Consequently depending on the ethylene content of an EP–MAH, there is usually less than 1 SAH per 100 backbone monomers and many techniques are not sensitive enough to probe the SAH moieties. The grafting of <sup>13</sup>C-labeled MAH onto polyolefins allows one to enhance the MAH signal so that <sup>13</sup>C NMR has been successfully used to investigate the nature of the MAH grafts of some EP–MAH samples.<sup>2</sup> However such an approach prevents the characterization of EP–MAH samples prepared without <sup>13</sup>C-labeled MAH. To circumvent this problem, the SAH moieties of already prepared EP–MAH can be reacted with a chromophore exhibiting an amine linker.<sup>3–7</sup> The outstanding sensitivity of fluorescence allows one to offset the low level of MAH grafting and gain information about the SAH moieties of EP–MAHs which have been selectively labeled.

One interesting characterization enabled by fluorescence is the direct determination of the extent of SAH

clustering in an EP–MAH sample.<sup>7</sup> We refer to this parameter as  $f_{\text{agg}}$  which represents the fraction of pendants which are aggregated in solution. The extent of SAH clustering or  $f_{\text{agg}}$  is an important parameter because it has a major effect on the viscosity of EP–MAH solutions in apolar solvents. Indeed a stronger clustering of SAH units along an EP–MAH sample has been shown to result in a steeper viscosity increase with increasing polymer concentration.<sup>7</sup> The determination of  $f_{\text{agg}}$  by fluorescence involves the labeling of an EP–MAH with 1-pyrenylmethylamine to yield a pyrene labeled EP copolymer (Py–EP), where pyrene is linked to the EP backbone via a rigid succinimide.<sup>3,4,7</sup> Upon irradiation with UV light, an excited pyrene can either emit fluorescence or encounter a ground-state pyrene to form an excited complex called an excimer. Time-resolved fluorescence measurements carried out on the pyrene monomer and excimer provide information on the extent of excimer formed either via diffusional encounters between two pyrenes or the direct excitation of an aggregate of ground-state pyrenes. If the excimer is found to be mostly formed via the direct excitation of ground-state pyrene aggregates, it indicates that the succinimide moieties bearing the pyrene pendants are clustered.

We have used this feature of the pyrene excimer fluorescence decays to determine quantitatively  $f_{\text{agg}}$  from the combined analysis of the monomer and excimer fluorescence decays of Py–EP samples.<sup>7</sup> The pyrene monomer and excimer decays of Py–EP were acquired in hexane and tetrahydrofuran (THF). These two solvents were chosen because hexane being apolar (dielectric constant:  $\epsilon = 1.89$ ) induced polar interactions between the succinimide pendants which led to the formation of pyrene aggregates, whereas THF being more polar ( $\epsilon = 7.52$ ) was able to reduce the associations between the succinimide moieties and the pyrene pen-

\* To whom correspondence should be addressed.

dants. As is demonstrated later on in this study, this result can also be predicted by comparing the solubility parameters of THF, hexane, and methyl succinimide. In any case, the analysis of the fluorescence decays presented in ref 7 successfully reflected the changes in pyrene aggregation associated with the polarity change of the solvent, which in turn validated the use of the proposed analysis.

In the present study, this analysis of the fluorescence decays is being implemented to demonstrate that the rather apolar solvent toluene ( $\epsilon = 2.38$ ) can melt the pyrene aggregates induced by the associations between the polar succinimide pendants of Py-EP as efficiently as the much more polar THF. This is a rather unexpected result if one considers the Hansen solubility parameters of toluene, which predict that methyl succinimide should be as poorly soluble in hexane or toluene. However this result should have important implications to rationalize the behavior of polymeric dispersants in oil for the following reasons. EP-MAH polymers can be reacted with polyamines to yield EP-NH<sub>2</sub> which are used as oil additives. In the oil, they act as colloidal stabilizers by having the amine-rich pendants adsorb onto the surface of polar particles which are generated during the operation of the engine. Once adsorbed, the polyolefin chain of EP-NH<sub>2</sub> stabilizes the particles in the oil. Although the hydrogen donor amines of EP-NH<sub>2</sub> induce strong interpolymeric associations in apolar oils,<sup>8,9</sup> the succinimide groups connecting the polyamine pendants to the EP backbone have been shown to generate strong polar associations on their own.<sup>10</sup> Since the efficiency of a dispersant depends on its ability to latch its polar substituents on the surface of the polar particles present in the oil, the polar succinimide linkers of EP-NH<sub>2</sub> contribute significantly toward the efficiency of these polymeric dispersants. Beside consisting essentially of long alkyl chains, motor oils do often contain a substantial fraction of aromatic compounds, sometimes up to 40 wt % of the total.<sup>11,12</sup> If aromatic compounds such as toluene can melt the associations taking place between the polar succinimide pendants of Py-EP, they are bound to also affect the efficiency of EP-NH<sub>2</sub> as a dispersant. Interestingly the effect of the content of aromatics in oil on the efficiency of EP-NH<sub>2</sub> at associating and forming polar aggregates has never been reported in the literature.

As a first step toward answering this question, we report herein how the presence of toluene in hexane affects the associations occurring between the succinimide pendants of Py-EP. In this study, toluene, hexane, and Py-EP are taken as model compounds that mimic the aromatics found in industrial oils, the saturated alkyl chains that constitute industrial oils, and an EP copolymer bearing succinimide moieties, respectively. Fluorescence experiments were performed as toluene was added to the hexane solution of Py-EP. The fluorescence experiments are used to determine how the fraction of aggregated pyrenes,  $f_{\text{agg}}$ , varies as a function of the toluene content in hexane. The parameter  $f_{\text{agg}}$  was determined using the analytical method described in ref 7. It provides a measure of the associative strength of Py-EP as a function of toluene content in hexane and its effect on the solution viscosity is monitored.

## Experimental Section

All instruments, techniques, and chemicals, beside spectrograde quality toluene purchased from EM Science, were

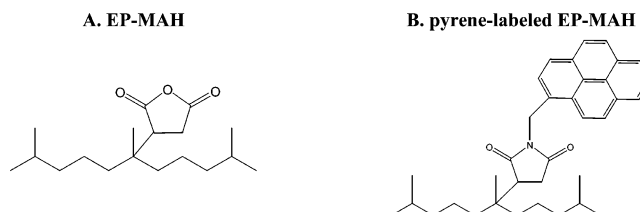


**Figure 1.** Chemical structure of EP-MAH (A) and pyrene-labeled EP-MAH (B).

**Table 1. Apparent Molecular Weight, Ethylene Content, and Level of MAH Grafting of EP-MAH**

polymer	$M_n$ (kg/mol)	$M_w/M_n$	ethylene (wt %)	MAH grafted ( $\mu\text{mol/g}$ of polymer)	no. of MAH grafts per chain
EP-MAH	28	2.8	49	151	4.2

**Table 2. Features of EP Copolymers Labeled with Pyrene (Py-EP) and Naphthalene (Np-EP)**

sample	chromophore content ( $\mu\text{mol/g}$ of polymer)	no. of ethylene and propylene units per label	mol % labeling
Py-EP	166	179	0.56
Np-EP	145	205	0.49

described in an earlier publication.<sup>7</sup> The chemical structure of the EP-MAH and Py-EP polymers is shown in Figure 1. Table 1 reports the molecular weight, polydispersity index, ethylene content, and level of MAH grafting of EP-MAH, whereas Table 2 describes the chromophore content of the labeled polymers.

**Analysis of the Fluorescence Decays.** The analysis of the fluorescence decays was performed by convoluting the theoretical equation of the fluorescence decays,  $g(t)$ , with the instrument response function. The presence of ground-state pyrene aggregates led to a fast process of excimer formation which could not be resolved accurately by our time-resolved fluorometer. Consequently a light scattering correction was applied to the analysis of the fluorescence decays to account for those fast events.<sup>13</sup> Different  $g(t)$  equations were used to fit the fluorescence decays. Qualitative information about the process of excimer formation could be obtained from fitting the decays with a sum of exponentials whose expression is given in eq 1. The number of exponentials,  $n$ , in eq 1 is varied from 1 to 4. The index  $X$  in eq 1 is either M or E, and it represents the monomer or the excimer, respectively. The parameters of  $g(t)$  were retrieved by using a least-squares curve fitting program based on the Marquardt-Levenberg algorithm.<sup>14</sup>

$$g(t) = \sum_{i=1}^{n} a_{Xi} e^{-t/\tau_{Xi}} \quad (1)$$

$X=M,E$

Quantitative information about the process of excimer formation was obtained by analyzing globally the monomer and excimer fluorescence decays with the blob model. In this analysis the monomer and excimer decays were fitted with eqs 2 and 4, respectively. Equation 2 was derived in an earlier paper<sup>15</sup> using Tachiya's mathematical treatment.<sup>16</sup>

$$[\text{Py}^*]_t = f_{\text{Mdiff}} \exp \left[ - \left( A_2 + \frac{1}{\tau_M} \right) t - A_3 (1 - \exp(-A_4 t)) \right] + (1 - f_{\text{Mdiff}}) \exp(-t/\tau_M) \quad (2)$$

The parameters  $A_2$ ,  $A_3$ , and  $A_4$  are described in eq 3.

$$A_2 = \langle n \rangle \frac{k_{\text{blob}} k_e [\text{blob}]}{k_{\text{blob}} + k_e [\text{blob}]} \quad A_3 = \langle n \rangle \frac{k_{\text{blob}}^2}{(k_{\text{blob}} + k_e [\text{blob}])^2} \quad A_4 = \frac{k_{\text{blob}} + k_e [\text{blob}]}{k_{\text{blob}} + k_e [\text{blob}]} \quad (3)$$

Equations 2 and 3 adopt the same expressions as those usually used to deal with pyrene excimer formation in micellar systems.<sup>17</sup>

Equation 2 is split into two exponentials. The first exponential is a stretched exponential which describes the time-dependent behavior of the fraction of pyrene monomers which forms excimer via diffusion,  $f_{\text{Mdiff}}$ . The second half of eq 2 handles the fraction,  $f_{\text{Mfree}} = 1 - f_{\text{Mdiff}}$ , of pyrene monomers which are isolated inside the polymer coil and cannot form excimer via diffusional encounter with a ground-state pyrene. These isolated pyrene monomers fluoresce with their natural lifetime,  $\tau_{\text{M}}$ . The parameters  $\langle n \rangle$ ,  $k_{\text{blob}}$ , and  $k_{\text{e}}[\text{blob}]$  refer to the average number of pyrene groups per blob, the rate constant of excimer formation inside a blob containing one excited pyrene and one ground-state pyrene only, and the rate at which pyrene groups exchange between blobs, respectively. Here,  $k_{\text{e}}$  is the exchange rate constant and  $[\text{blob}]$  is the blob concentration inside the polymer coil.

The fit of the excimer decays with eq 4 requires assuming the existence of three pyrene species. These species are  $[\text{Py}_{\text{diff}}^*]_{(t=0)}$ ,  $[\text{E0}^*]_{(t=0)}$ , and  $[\text{D}^*]_{(t=0)}$  which represent the equilibrium concentrations of the pyrenes which form excimer via diffusion, are preassociated and form an excimer upon direct excitation, and are preassociated and form a long-lived excimer upon absorption of a photon, respectively. The lifetimes of  $\text{E0}^*$  and  $\text{D}^*$  are  $\tau_{\text{E0}}$  and  $\tau_{\text{D}}$ , respectively, and they were optimized. The monomer lifetime,  $\tau_{\text{M}}$ , was fixed in the analysis to that of an oligoisobutylene model compound that bore a 1-pyrenemethylsuccinimide moiety at one end of the chain.<sup>18</sup> The Marquardt–Levenberg algorithm is applied to retrieve the parameters  $A_2$ ,  $A_3$ , and  $A_4$  from the fit of the fluorescence decays.<sup>14</sup> The global fit of the monomer and excimer decays was considered good if the  $\chi^2$  parameter was less than 1.30 and if the residuals and the autocorrelation function of the residuals were randomly distributed around zero.

$$[\text{E}^*] = -[\text{Py}_{\text{diff}}^*]_{(t=0)} e^{-A_3 \sum_{i=0}^{\infty} \frac{A_3^i}{i!} \frac{A_2 + iA_4}{\frac{1}{\tau_{\text{M}}} - \frac{1}{\tau_{\text{E0}}} + A_2 + iA_4}} \times \exp\left(-\left(\frac{1}{\tau_{\text{M}}} + A_2 + iA_4\right)t\right) + \left([\text{E0}^*]_{(t=0)} + [\text{Py}_{\text{diff}}^*]_{(t=0)} e^{-A_3 \sum_{i=0}^{\infty} \frac{A_3^i}{i!} \frac{A_2 + iA_4}{\frac{1}{\tau_{\text{M}}} - \frac{1}{\tau_{\text{E0}}} + A_2 + iA_4}}\right) e^{-t/\tau_{\text{E0}}} + [\text{D}^*]_{(t=0)} e^{-t/\tau_{\text{D}}} \quad (4)$$

## Results and Discussion

The syntheses of EP labeled with 1-pyrenemethylamine (Py-EP) and with 1-naphthalenemethylamine (Np-EP) used in the present study have been described in an earlier publication.<sup>7</sup> The dye content averaged over all polymers equalled  $154 \pm 9 \mu\text{mol}$  of chromophore per gram of polymer. The number-average molecular weight and polydispersity of Py-EP ( $M_n$ ) were determined by GPC to equal 41 kg/mol and 3.0, respectively. Table 2 lists the features of the labeled EP samples.  $M_n$  of Py-EP is larger than that of the naked EP ( $M_n = 28\text{K}$ , cf. Table 1) because of the successive precipitations performed during the work up procedure after the labeling reaction.

**UV–Vis Absorption.** The UV–vis absorption spectra of Py-EP were acquired in mixtures of hexane and toluene of various compositions. Absorption measurements provide qualitative information about the level of association between pyrene pendants. A broadening

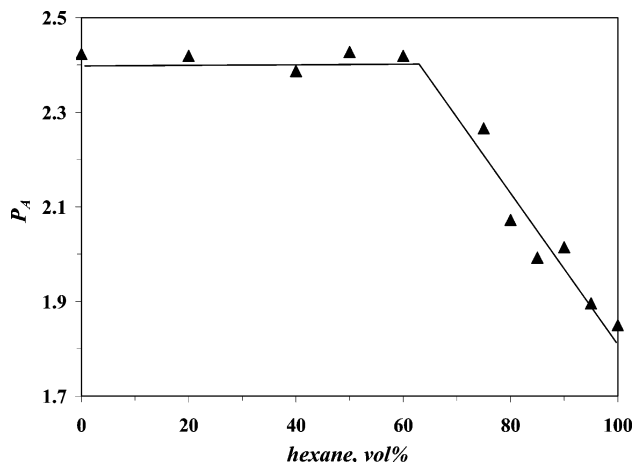


**Figure 2.**  $P_A$  values of Py-EP as a function of the volume fraction of hexane in the hexane/toluene mixtures.

of the absorption bands is usually observed as a result of pyrene association.<sup>19</sup> The peak-to-valley ratio,  $P_A$ , provides a measure of this broadness by measuring the ratio of the absorbance of the peak at 344 nm to that of the nearest valley. A  $P_A$  value of 3.0 or above indicates absence of association whereas a lower value indicates increased pyrene association. In hexane, the  $P_A$  value equals 1.85 which suggests strong association of the pyrene groups. As shown in Figure 2, the  $P_A$  value increases with decreasing hexane content until it plateaus at  $2.4 \pm 0.0$  for hexane volume fractions smaller than 60 vol %.

These results indicate that toluene can melt the pyrene aggregates originally formed in hexane. However, the inherent existence of clustered SAH pendants in EP-MAH generated during the maleation of the EP copolymer leads to clustered pyrene pendants (or pyrene aggregates) when the EP-MAH is labeled with 1-pyrenemethylamine.<sup>7</sup> Consequently, even at toluene contents exceeding 40 vol %, the  $P_A$  value equals  $2.4 \pm 0.0$ , a value lower than the ideal  $P_A$  value of 3.0 which would indicate the complete absence of ground-state (GS) pyrene aggregates. The residual pyrene association observed in toluene will be discussed in further details later.

There are two possible origins for the GS pyrene aggregates observed in hexane. The GS pyrene aggregates can be due to dipolar associations between the polar succinimide groups linking the pyrenyl moieties to the EP backbone or the poor solubility of the aromatic pyrenes in hexane. To address this question, the carbonyl functions of the succinimide pendants of Py-EP were reduced using  $\text{LiAlH}_4$  to yield a much less polar *N*-substituted pyrrolidine unit as the linker of the pyrenyl pendants to the EP copolymer. These experiments are to be described in detail in a forthcoming publication.<sup>20</sup> In hexane, the  $P_A$  value jumped from 1.9 to 2.8 before and after reduction, respectively. In contrast, the  $P_A$  value in THF varied very slightly from 2.7 to 2.9 before and after reduction, respectively. These results led to the conclusion that the reduction of the carbonyl groups strongly decreases the level of association between the pyrene groups in hexane and that the main drive toward the aggregation of the pyrene pendants of Py-EP in hexane is the polar interactions taking place between the succinimide moieties.

**Steady-State Fluorescence Measurement.** When a Py-EP solution is excited by UV light, the pyrene



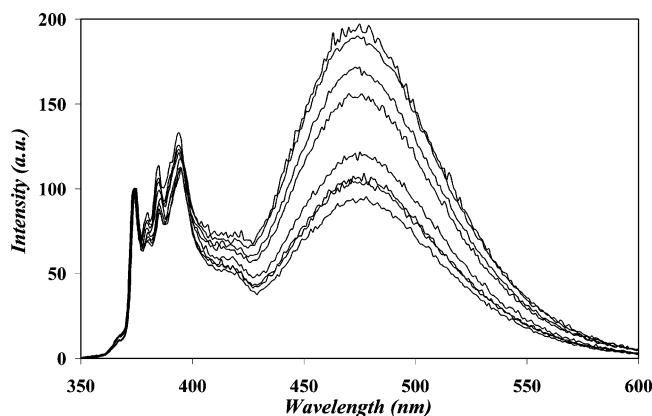


**Figure 3.** Fluorescence emission spectra of Py-EP in hexane/toluene mixtures. The excimer emission centered near 480 nm increases with hexane content in the solvent mixture (bottom trace, toluene; top trace, hexane). [Py-EP] =  $2.5 \times 10^{-6}$  M,  $\lambda_{\text{ex}}$  = 344 nm for all samples except 346 nm for the sample in toluene.

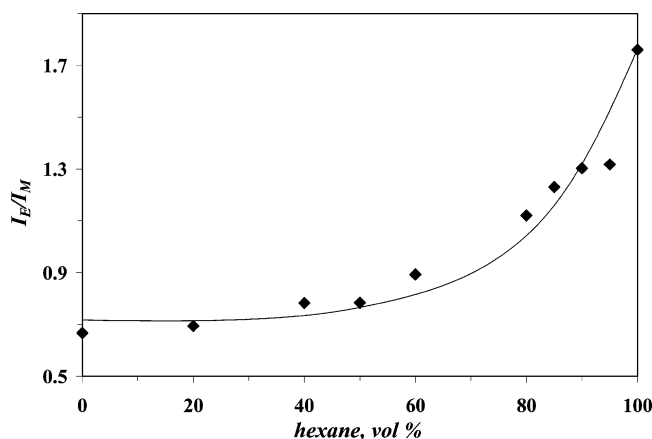


**Figure 4.**  $I_E/I_M$  of Py-EP at various volume fractions of hexane in the hexane/toluene mixtures.

monomer can fluoresce with its natural lifetime,  $\tau_M$ , or it can form an excimer upon encounter with a GS pyrene. Figure 3 shows the typical fluorescence emission spectra of Py-EP as a function of solvent composition. The pyrene monomer fluorescence emission exhibits sharp peaks between 370 and 410 nm, whereas that of the excimer is broad, structureless, and centered around 480 nm. Since the process of excimer formation depends on the average distance separating any two pyrene units attached on the polymer, an increased excimer formation indicates that the pyrene units are closer to one another. Figure 3 demonstrates that increasing the hexane content in the mixtures yields enhanced excimer formation. This can be represented in a more quantitative manner by plotting in Figure 4 the  $I_E/I_M$  ratio as a function of solvent composition. The  $I_E/I_M$  ratio represents the ratio of the excimer fluorescence intensity taken by integrating the area under the fluorescence emission spectrum from 500 to 530 nm over the monomer fluorescence intensity taken by integrating the area under the fluorescence spectrum from 372 to 378 nm. The plot shown in Figure 4 indicates that toluene hinders the formation of excimer. If the  $I_E/I_M$  value of 1.76 and 0.6, respectively obtained in hexane and toluene, are taken as the two  $I_E/I_M$  extremes, adding 25 vol % of toluene decreases the  $I_E/I_M$  ratio by about 70%. Toluene appears to be very efficient at preventing the formation of excimer by melting the polar aggregates

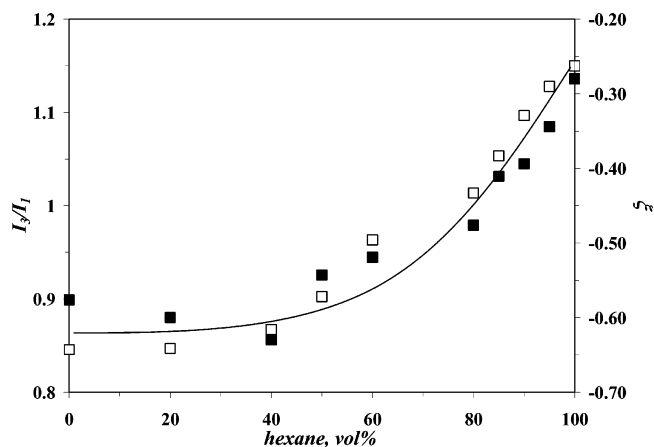


**Figure 5.**  $I_3/I_1$  ( $\square$ ) and  $\xi$  ( $\blacksquare$ ) of Py-EP obtained at various volume fractions of hexane in hexane/toluene mixtures.

existing in hexane between the succinimide pendants as inferred by the absorption measurements (cf. Figure 2).

One typical mode of excimer formation is by the diffusional encounters of two pyrenes attached onto the backbone. Because toluene ( $\eta$  = 0.560 mPa.s at 25 °C) is more viscous than hexane ( $\eta$  = 0.300 mPa.s at 25 °C) at room temperature, the decrease of excimer formation observed upon toluene addition might be due to a reduction of excimer formation via diffusion. Yet the time-resolved fluorescence measurements presented later demonstrate that this is not the case and that the formation of excimer via diffusion is actually enhanced upon adding toluene to the solution.

The existence of pyrene aggregates observed in hexane and their disappearance upon adding toluene can be further confirmed by acquiring fluorescence excitation spectra.<sup>19</sup> Excitation spectra of Py-EP were obtained using an emission wavelength of 375 and 500 nm for the pyrene monomer and excimer, respectively. They are shown in Figure SI.1 in the Supporting Information for Py-EP in hexane (top) and toluene (bottom). A shift between the monomer and excimer excitation spectra indicates the presence of ground-state pyrene dimers.<sup>19</sup> Since noticeable shifts between the monomer and excimer excitation spectra are observed in hexane and not in toluene, more GS pyrene dimers are present in hexane than in toluene, a conclusion similar to the one drawn from Figure 2.

Although the fluorescence spectrum of a pyrene molecule is known to provide information about the polarity of its microenvironment by measuring the  $I_3/I_1$  ratio of the third ( $I_3$ ) to the first ( $I_1$ ) vibronic band of the fluorescence spectrum, this effect is usually much less pronounced with pyrenyl pendants such as those of Py-EP.<sup>21</sup> Nevertheless there have been several examples in the literature where the  $I_3/I_1$  ratio of pyrene labeled polymers has been reported in order to provide information about the micropolarity of the environment surrounding the pyrenyl pendants.<sup>22–32</sup> When the  $I_3/I_1$  ratio is recorded in Figure 5 as a function of the hexane content of the mixtures, it shows a significant increase from 0.85 in toluene up to 1.15 in hexane. This is a rather unexpected result because the  $I_3/I_1$  ratio is supposed to depend on the polarity of the microenvironment experienced by the pyrenyl pendant. Since the polarity of hexane and toluene is similar, the two apolar solvents having a dielectric constant of 1.89 and 2.38, respectively, the pyrenyl pendant in toluene must be

probing the polar succinimide moieties. The  $I_3/I_1$  trend shown in Figure 5 implies that toluene favors interactions between the pyrene and the succinimide moieties.

It is also worth noting that the change of the  $I_3/I_1$  ratio is not due to the presence or absence of ground-state pyrene aggregates since the exact same trend is obtained for an oligoisobutylene terminated at one end with a maleic anhydride and labeled with 1-pyrenemethylamine (Py-OIB).<sup>18</sup> Py-OIB does not form intermolecular pyrene aggregates at low polymer concentration, yet the  $I_3/I_1$  ratio obtained for Py-OIB matches exactly that of Py-EP (data not shown), thus demonstrating that the effect shown in Figure 5 does not result from the formation of ground-state pyrene aggregates.

**Time-Resolved Fluorescence Measurement.** The monomer and excimer fluorescence decays of Py-EP were acquired. Sums of four and three exponentials were required to fit the monomer and excimer fluorescence decays. In the analysis of the monomer decays, the fourth decay time was fixed to that of Py-OIB.<sup>18</sup> The results of the fits are listed in Table SI.1 in the Supporting Information. In the case of the excimer decays, the ratio  $\xi = a_{e1}/(a_{e2} + a_{e3})$  can yield information about the formation mechanism of the pyrene excimer. If no ground-state dimer is present,  $\xi$  equals  $-1.0$ . On the contrary, if all pyrene excimers are formed via ground-state dimers,  $\xi$  equals  $0.0$ . For a typical solution of a pyrene labeled polymer, both mechanisms are involved. Consequently,  $\xi$  takes a value between  $-1.0$  and  $0.0$ , depending on the fraction of pyrene excimer formed by one mechanism against the other. A more positive  $\xi$  value indicates that more pyrene units are preassociated.

As shown in Figure 5, the  $\xi$  value of Py-EP changes gradually from  $-0.58$  to  $-0.28$  when the solvent is progressively switched from toluene to hexane. This indicates that more pyrene excimers are formed via diffusional encounters in toluene than in hexane or that more pyrene aggregates exist in hexane than in toluene. As mentioned previously, since hexane is a poor solvent for the polar succinimide groups, it induces dipolar associations between the succinimide moieties, which draw the pyrene groups together. Toluene seems to be a better solvent for both the polar succinimide and the pyrene pendants reducing the amount of pyrene aggregates (cf. Figures 2 and SI.1). The  $\xi$  value never equals  $-1.0$  because the labeling of EP-MAH with 1-pyrenemethylamine reflects the inherent SAH clustering along EP-MAH and the pyrene pendants end up being clustered as well.<sup>7</sup> Upon direct excitation, the pyrene clusters behave as pyrene aggregates and the  $\xi$  ratio does not equal  $-1.0$  so that a  $\xi$  value of  $-1.0$  was never obtained even in toluene. The fluorescence decay measurements confirm the previous observations made with the UV-vis absorption (cf. Figure 2) and the fluorescence excitation measurements (cf. Figure SI.1), namely that the associations between the succinimide moieties and the pyrene pendants are much stronger in hexane than in toluene.

As the volume fraction of hexane decreases, the  $\xi$  value becomes more negative as a result of the increasing amount of pyrene excimers being formed via diffusion when the toluene content increases. Furthermore, it is interesting to note that 25 vol % of toluene reduces the  $\xi$  value by 60% from its value in hexane to its value in toluene. Further increase of the toluene content yields even more negative  $\xi$  values and a plateau is reached

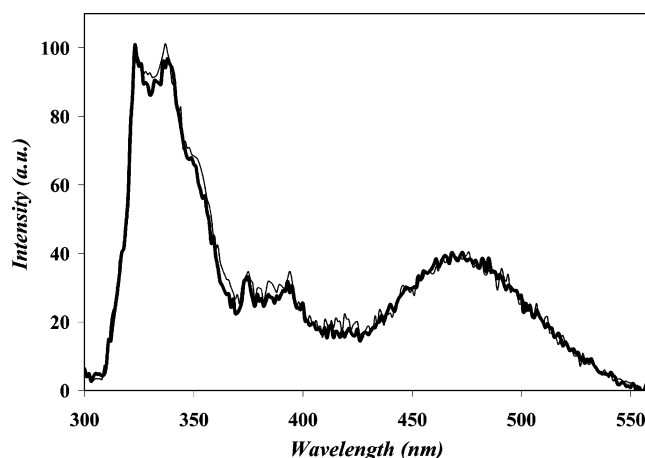


**Figure 6.** Emission spectra of mixing experiment in hexane/toluene mixture with a hexane content of 40 vol % ( $\lambda_{\text{ex}} = 290$  nm). (i) mixed solution of Py-EP and Np-EP (—) and (ii) addition of the fluorescence spectrum of Py-EP alone with that of Np-EP alone (---). Concentrations:  $2.5 \times 10^{-6}$  M for Py-EP,  $2.3 \times 10^{-5}$  M for Np-EP.

for volume fractions of hexane smaller than 40 vol % (cf. Figure 5). These results demonstrate that relatively small amounts of toluene are very efficient at breaking up the pyrene aggregates formed in hexane. It is interesting to note in Figure 5 that both  $\xi$  and  $I_3/I_1$  values show a very similar trend when they are plotted against the hexane fraction. Since these parameters probe two different aspects of a Py-EP/solvent system, i.e., pyrene aggregation and chromophore micropolarity for  $\xi$  and  $I_3/I_1$ , respectively, it suggests that the two effects are correlated. However no rationale has been found to explain this correlation.

**Fluorescence Resonance Energy Transfer (FRET).** The complete characterization of an associative polymer requires determining whether the associations take place within one polymer chain or between different chains, namely intramolecular vs intermolecular interactions. To this end, fluorescence resonance energy transfer (FRET) experiments were carried out. FRET has been used extensively in biological studies as a “spectroscopic ruler”, due to the strong dependence of the FRET efficiency on the distance separating the donor from its acceptor.<sup>33,34</sup> It has also been widely applied to study polymeric systems.<sup>7,23,28,35–42</sup> The dyes chosen for the FRET experiments were naphthalene and pyrene. The naphthalene/pyrene pair is frequently used for FRET experiments where the donor naphthalene can be excited selectively and can transfer its excess energy to the ground-state pyrene.<sup>7,23,28,43–46</sup>

FRET was used to determine whether intra- or intermolecular interactions occur between the labeled EPs. In these experiments, the emission spectra are acquired for solutions containing Py-EP only, Np-EP only, and a mixture of the two. The solutions were prepared so that the concentration of pyrene or naphthalene would equal  $2.5 \times 10^{-6}$  or  $2.3 \times 10^{-5}$  M, respectively. When the mixed solution of Py-EP and Np-EP was excited at 290 nm, an emission spectrum with a very weak contribution from the pyrene monomer (emission at 374 nm) and a strong contribution from naphthalene (emission at 330 nm) was obtained (cf. Figure 6). The comparison of this emission spectrum with the sum of the individual spectra of Py-EP and Np-EP shows no difference, confirming that no FRET occurs between two chromophores located on different

chains in a solvent mixture containing 40 vol % of hexane. In other words, FRET occurs intramolecularly.

A similar conclusion had been reached earlier in hexane for the same Py-EP and Np-EP samples, where the chromophores had been found to aggregate intramolecularly.<sup>7</sup> Since no intermolecular aggregation of the chromophores could be detected by FRET in hexane where the chromophores are aggregated (cf. Figures 2, SI.1, and 5) or in a mixture containing 40 vol % of hexane where the chromophores show much less aggregation (cf. Figures 2 and 5), it can be concluded that no interchain interactions occur for the polymer/solvent system used in the fluorescence experiments presented in this report.

**Determination of the Association Level by FBM Global Analysis.** The experiments carried out so far have demonstrated that the addition of toluene to hexane decreases the level of intramolecular associations between the pyrene pendants of Py-EP. These trends can be quantified by determining the fraction of aggregated pyrenes as a function of the hexane content in the hexane/toluene mixtures. This is done by analyzing the fluorescence decays with the fluorescence blob model (FBM). So far, the FBM has been successfully employed to determine the level of association of pyrene labeled associative polymers,<sup>5-7,43-46</sup> the dynamics of polymer chains,<sup>15,47</sup> and the polymer coil size change undergone during the coil-globule transition.<sup>48,49</sup> The FBM was introduced to account for the distribution of excimer formation rate constants, which results from the random labeling of pyrene units along a polymeric backbone. In a global analysis with the FBM, the fluorescence decays of the pyrene monomer and excimer are fitted simultaneously to ensure that some of the parameters used in the analysis are held the same in both the monomer and excimer decays. The advantage of performing a global analysis on the fluorescence decays is that the parameters retrieved from the analysis are obtained with higher accuracy.<sup>50,51</sup> The FBM global analysis was performed on the fluorescence decays of Py-EP acquired in mixtures of hexane and toluene at various solvent compositions.

In a typical FBM global analysis, monomer and excimer decays are fitted with eqs 2 and 4, respectively. The parameters  $f_{\text{Mdiff}}$ ,  $f_{\text{Mfree}}$ ,  $k_{\text{blob}}$ ,  $\langle n \rangle$ , and  $k_{\text{e[blob]}}$  retrieved from the analysis of the monomer decays are listed in Table SI.2A in the Supporting Information. The fluorescence lifetime ( $\tau_{\text{M}}$ ) of the pyrene monomer was fixed in the analysis to equal that of Py-OIB whose fluorescence decay was acquired at the same solvent composition. The lifetimes of the excimer  $\text{E0}^*$  ( $\tau_{\text{E0}}$ ) and the long-lived low energy excited dimers  $\text{D}^*$  ( $\tau_{\text{D}}$ ) used in eq 4 were optimized in the global analysis of the monomer and excimer decays. For all the pyrene monomers present in solution and probed by the fluorescence decays of the monomer, the parameter  $f_{\text{Mdiff}}$  denotes the fraction of pyrene monomers forming excimer via diffusion ( $\text{Py}_{\text{diff}}^*$ ) while  $f_{\text{Mfree}}$  ( $= 1 - f_{\text{Mdiff}}$ ) denotes the fraction of pyrene monomers which are isolated ( $\text{Py}_{\text{free}}^*$ ). The parameters  $\langle n \rangle$ ,  $k_{\text{diff}}$ , and  $k_{\text{e[blob]}}$  have been defined in the Experimental section. They model the diffusive encounters between an excited pyrene and a ground-state pyrene or pyrene dimer. The parameters  $k_{\text{blob}}$ ,  $\langle n \rangle$ , and  $k_{\text{e[blob]}}$  are found in eqs 2 and 4 and are held the same during the global analysis of the monomer and excimer decays. The fractions  $f_{\text{Ediff}}$ ,  $f_{\text{EEO}}$ , and  $f_{\text{ED}}$  retrieved from the analysis of the excimer

decays with eq 4 characterize the species  $\text{Py}_{\text{diff}}^*$ ,  $\text{E0}^*$ , and  $\text{D}^*$ , respectively. Their values are listed in Table SI.2A.

Quantitative information about the fraction of aggregated pyrenes is obtained from the fractions  $f_{\text{diff}}$ ,  $f_{\text{free}}$ ,  $f_{\text{E0}}$ , and  $f_{\text{D}}$  which are calculated from  $f_{\text{Mdiff}}$ ,  $f_{\text{Mfree}}$ ,  $f_{\text{Ediff}}$ ,  $f_{\text{EEO}}$ , and  $f_{\text{ED}}$  according to eq 5, parts a-d. The parameters  $f_{\text{diff}}$ ,  $f_{\text{free}}$ ,  $f_{\text{E0}}$ , and  $f_{\text{D}}$  represent the fractions of pyrene monomers  $\text{Py}_{\text{diff}}^*$ ,  $\text{Py}_{\text{free}}^*$ ,  $\text{E0}^*$ , and  $\text{D}^*$ , respectively. The fraction of associated pyrene units ( $f_{\text{agg}}$ ) is obtained by summing  $f_{\text{E0}}$  and  $f_{\text{D}}$ . The validity of the blob model has been demonstrated for various polymers randomly labeled with pyrene over the past few years.<sup>5-7,15,43-49</sup>

$$f_{\text{diff}} = \frac{[\text{Py}_{\text{diff}}^*]_{(t=0)}}{[\text{Py}_{\text{diff}}^*]_{(t=0)} + [\text{Py}_{\text{free}}^*]_{(t=0)} + [\text{E0}^*]_{(t=0)} + [\text{D}^*]_{(t=0)}} = \left( 1 + \frac{f_{\text{Mfree}}}{f_{\text{Mdiff}}} + \frac{f_{\text{EEO}}}{f_{\text{Ediff}}} + \frac{f_{\text{ED}}}{f_{\text{Ediff}}} \right)^{-1} \quad (5a)$$

$$f_{\text{free}} = \frac{[\text{Py}_{\text{free}}^*]_{(t=0)}}{[\text{Py}_{\text{diff}}^*]_{(t=0)} + [\text{Py}_{\text{free}}^*]_{(t=0)} + [\text{E0}^*]_{(t=0)} + [\text{D}^*]_{(t=0)}} = f_{\text{diff}} \times \frac{f_{\text{Mfree}}}{f_{\text{Mdiff}}} \quad (5b)$$

$$f_{\text{E0}} = \frac{[\text{E0}^*]_{(t=0)}}{[\text{Py}_{\text{diff}}^*]_{(t=0)} + [\text{Py}_{\text{free}}^*]_{(t=0)} + [\text{E0}^*]_{(t=0)} + [\text{D}^*]_{(t=0)}} = f_{\text{diff}} \times \frac{f_{\text{EEO}}}{f_{\text{Ediff}}} \quad (5c)$$

$$f_{\text{D}} = \frac{[\text{D}^*]_{(t=0)}}{[\text{Py}_{\text{diff}}^*]_{(t=0)} + [\text{Py}_{\text{free}}^*]_{(t=0)} + [\text{E0}^*]_{(t=0)} + [\text{D}^*]_{(t=0)}} = f_{\text{diff}} \times \frac{f_{\text{ED}}}{f_{\text{Ediff}}} \quad (5d)$$

The fits obtained from the global analysis of the monomer and excimer decays were good, since the  $\chi^2$  values were always smaller than 1.30 and the residuals and the autocorrelation function of the residuals were randomly distributed around zero. The parameters retrieved from the analyses are listed in Table SI.2A. Within experimental error, all monomer fluorescence decays yielded similar parameters for all solvent compositions with  $f_{\text{Mfree}}$ ,  $f_{\text{Mdiff}}$ ,  $\langle n \rangle$ ,  $k_{\text{blob}}$ , and  $k_{\text{e[blob]}}$  found to equal  $0.18 \pm 0.03$ ,  $0.82 \pm 0.03$ ,  $1.48 \pm 0.05$ ,  $(2.1 \pm 0.3) \times 10^7 \text{ s}^{-1}$ , and  $(5.4 \pm 0.5) \times 10^6 \text{ s}^{-1}$ , respectively. The lifetime  $\tau_{\text{E0}}$  was found to decrease continuously from 64 ns in hexane to 52 ns in toluene. These  $\tau_{\text{E0}}$  values are reasonable since Py-EP has been found to yield  $\tau_{\text{E0}}$  values equal to  $56 \pm 1$  and  $61 \pm 1$  ns in THF and hexane, respectively.<sup>7</sup>

The fractions  $f_{\text{diff}}$ ,  $f_{\text{free}}$ ,  $f_{\text{E0}}$ ,  $f_{\text{D}}$ , and  $f_{\text{agg}}$  ( $f_{\text{agg}} = f_{\text{E0}} + f_{\text{D}}$ ) of all pyrene species were calculated and are listed in Table SI.2B. The most noticeable change is observed for  $f_{\text{diff}}$  and  $f_{\text{agg}}$  which, respectively, double and halve when the solvent is switched from hexane to toluene. It indicates that much less pyrene aggregates are present in toluene than in hexane. Since hexane is a nonpolar



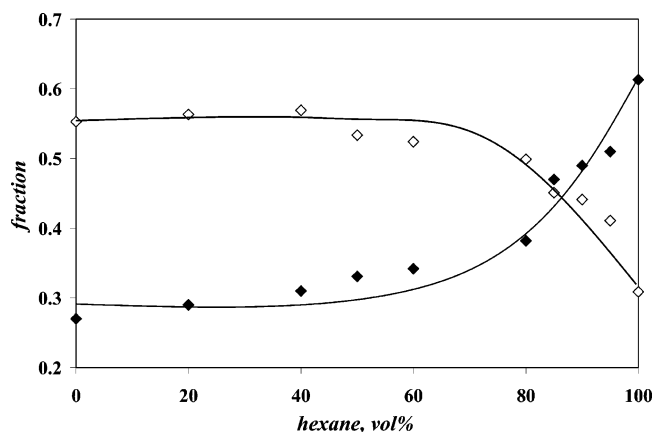


**Figure 7.** Fractions of pyrene species at various hexane volume fractions,  $f_{\text{diff}}$  ( $\diamond$ ) and  $f_{\text{agg}}$  ( $\blacklozenge$ ).

alkyl chain solvent, it induces dipolar associations between the succinimide moieties and  $\pi$ -stacking between the aromatic pyrenes. The fractions  $f_{\text{diff}}$  and  $f_{\text{agg}}$  are plotted as a function of the volume fraction of hexane in Figure 7.  $f_{\text{agg}}$  is found to decrease rapidly upon relatively small additions of toluene to hexane.  $f_{\text{agg}}$  remains constant for hexane volume fractions smaller than 60 vol % and equals  $0.31 \pm 0.02$ . The profile of  $f_{\text{agg}}$  is mirrored by that of  $f_{\text{diff}}$ .  $f_{\text{diff}}$  increases rapidly upon small additions of toluene to hexane followed by a plateau with an average value of  $0.55 \pm 0.02$  when the hexane volume fraction is smaller than 60 vol %.

In addition, the onset of the plateau for both parameters occurred at the same hexane volume fraction, i.e., 60 vol %. It indicates that the decrease in  $f_{\text{agg}}$  is a direct consequence of the increase in  $f_{\text{diff}}$  when the toluene content increases. Here again the inherent clustering of the succinic anhydride moieties along the EP–MAH backbone prevents the complete melting of the pyrene aggregates and  $f_{\text{agg}}$  never equals zero even in toluene.<sup>7</sup> These results confirm quantitatively that toluene is very effective at loosening the polar associations taking place between succinimide moieties in hexane. More importantly, the trends obtained from the quantitative determination of  $f_{\text{agg}}$  as a function of the hexane volume fraction are in very good agreement with those obtained with the  $P_A$ ,  $I_E/I_M$ , and  $\xi$  ratios, shown in Figures 2, 4, and 5, respectively.

**Comparison of the Solubility of Methyl Succinimide in THF, Toluene, and Hexane.** All the results obtained by fluorescence suggest that addition of toluene to a solution of Py–EP in hexane melts the polar interactions that exist between the succinimide pendants. To further illustrate that this is a rather unexpected result, the solubility of methyl succinimide in THF, toluene, and hexane was estimated by using the Hansen solubility parameters. When doing so, the Hildebrand solubility parameter,  $\delta$ , is decomposed into three contributions which represent the London dispersion forces,  $\delta_d$ , the permanent dipole–dipole interactions,  $\delta_p$ , and the hydrogen bonding forces,  $\delta_h$ . The solubility parameters  $\delta$ ,  $\delta_d$ ,  $\delta_p$ , and  $\delta_h$  are related to one another via eq 6.<sup>52</sup>

$$\delta^2 = \delta_d^2 + \delta_p^2 + \delta_h^2 \quad (6)$$

The values of the solubility parameters are listed in Table 3.

In Table 3, the solubility parameters  $\delta$ ,  $\delta_d$ ,  $\delta_p$ , and  $\delta_h$  for methyl succinimide were estimated (more details

**Table 3.** Solubility Parameters  $\delta$ ,  $\delta_d$ ,  $\delta_p$ , and  $\delta_h$  and the Distance between Solvent and Solute Coordinates  $R_{ij}$  where i Stands for Methyl Succinimide and j Stands for THF, Toluene, and Hexane

compound	$\delta$ (MPa <sup>1/2</sup> )	$\delta_d$ (MPa <sup>1/2</sup> )	$\delta_p$ (MPa <sup>1/2</sup> )	$\delta_h$ (MPa <sup>1/2</sup> )	$R_{ij}$ (MPa <sup>1/2</sup> )
methyl succinimide	20.6	15.6	9.6	9.5	
THF	19.5	16.8	5.7	8	4.8
toluene	18.2	18	1.4	2	12.1
hexane	14.9	14.9	0	0	13.6

about this calculation are given in the Supporting Information), whereas those of THF, toluene, and hexane were found in the literature.<sup>53</sup> According to the Hildebrand solubility parameter,  $\delta$ , THF and toluene should solubilize any compound with a similar efficiency, since their  $\delta$ 's take comparable values. This is because the Hildebrand solubility parameters do not account for the dipolar and hydrogen bonding forces. When those are taken into account with the Hansen parameters, the efficiency of a given solvent at solubilizing methyl succinimide is obtained with the  $R_{ij}$  parameter which measures the distance between the solvent and solute coordinates. The expression of  $R_{ij}$  is given in eq 7.<sup>52</sup>  $R_{ij}$  was calculated for each solvent/solute pair and its values are listed in the sixth column of Table 3.

$$R_{ij} = \{4 \times (\delta_{id} - \delta_{jd})^2 + (\delta_{ip} - \delta_{jp})^2 + (\delta_{ih} - \delta_{jh})^2\}^{1/2} \quad (7)$$

According to the  $R_{ij}$  values, THF is a much better solvent for methyl succinimide than both toluene and hexane, which exhibit similar  $R_{ij}$  values and should both solubilize methyl succinimide poorly. These calculations confirm that THF, being more polar, is expected to solubilize succinimide pendants better than apolar solvents like hexane and more surprisingly toluene, contrarily to what has been observed experimentally by fluorescence in the present study.

**Viscosity of EP Copolymer Solutions.** Maleated EP copolymers are widely used as viscosity improvers in engine oils.<sup>8</sup> Their performance is expected to depend strongly on the engine oil components. Many oils contain a substantial fraction of aromatics.<sup>11,12</sup> Our fluorescence studies indicate that additions of toluene to hexane, i.e., additions of an aromatic molecule to an alkane solvent, reduce the fraction of associated pendants of Py–EP. It becomes thus interesting to investigate whether the reduction of association induced by the addition of toluene affects the rheological behavior of the Py–EP solution.

To do so, the solution viscosity of both naked EP and Py–EP was measured as a function of polymer concentration in toluene, hexane, and a mixture of the two. Figure 8 shows that the solution viscosity of both EP samples increases with increasing polymer concentration regardless of solvent. It must be noted that the viscosity measurements are performed at polymer concentrations larger than 1 g/L, i.e., at least five times larger than the EP concentrations used for the FRET experiments performed in Figure 6 and 50 times larger than the Py–EP concentrations used in Figures 2–5 and 7. The Py–EP sample exhibits a much steeper viscosity increase in hexane than in toluene. This behavior can be attributed to the formation of interpolymeric aggregates which is promoted in hexane via dipolar interactions between the succinimide pendants and hindered in toluene.

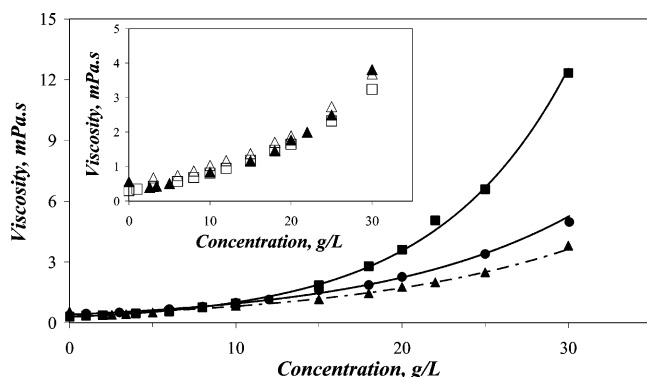


**Figure 8.** Viscosity of Py-EP and naked EP. Py-EP in hexane (■), toluene (▲), and hexane/toluene mixture (70 vol % hexane) (●); naked EP in hexane (□) and toluene (△).

In contrast, the naked EP sample yields very similar profiles in both solvents (cf. inset in Figure 8). This is because hexane and toluene do not promote the formation of interpolymeric aggregates for the EP copolymers used in this study, as inferred from the FRET experiment shown in Figure 6 for a mixture of hexane and toluene and performed in hexane only in an earlier publication.<sup>7</sup> Therefore, the viscosity increase of the naked EP in both solvents with polymer concentration is much more modest than that of Py-EP in hexane while it is close to that of Py-EP in toluene. This result suggests that the pendants of Py-EP have no effect on the rheological behavior of Py-EP in toluene. It is interesting to note that, when the Py-EP was dissolved in a hexane/toluene mixture with a hexane content of 70 vol %, the viscosity increase of that solution with polymer concentration is much reduced with respect to that found in hexane. In fact, the viscosity-vs-concentration profile of Py-EP in the mixture is, to some extent, very close to that of the naked EP in either solvent (cf. inset of Figure 8). This result furthers the conclusion made earlier that the presence of toluene hinders the formation of inter-polymeric aggregates which leads to a significant decrease in solution viscosity. These results demonstrate that the polar succinimide moieties are accountable for the interesting rheological behavior of Py-EP observed in hexane and that toluene contributes to the melting of the polar associations occurring in hexane.

## Conclusions

A maleated EP copolymer was labeled with 1-pyrenemethylamine. The fluorescence properties of Py-EP were studied in solvent mixtures consisting of hexane and toluene at various compositions. UV-vis absorption and steady-state and time-resolved fluorescence measurements were performed on Py-EP, which all led to the conclusions that toluene can melt the polar associations induced by the succinimide moieties in hexane and that a small amount of toluene can significantly decrease the polar associations. A mixture containing 25 vol % toluene leads to a decrease of 68%, 60%, and 71% in  $I_F/I_M$ ,  $\xi$ , and  $f_{agg}$ , respectively, from their value in hexane to their value in toluene. FRET experiments carried out with Py-EP and Np-EP demonstrated that no intermolecular interactions occur at the polymer concentrations used in the fluorescence experiments.

Global analyses with the FBM were carried out on the monomer and excimer fluorescence decays of Py-EP to determine quantitatively the fraction of ag-

gregated pyrenes at different hexane volume fractions of the solvent mixture. By switching the solvent from hexane to toluene, the fraction of aggregated pyrenes dropped from 61% in hexane to 29% in toluene. The fraction of aggregated pyrenes decreased gradually with decreasing hexane content in the hexane/toluene mixtures until it reached a plateau at a hexane volume fraction of 60 vol %.

The viscosity of the naked EP and Py-EP solutions was measured in hexane, toluene, and a mixture containing 70 vol % of hexane. The viscosity-vs-concentration profile of Py-EP exhibited a much steeper increase in hexane than in toluene while the naked EP did not display such a strong dependence of the viscosity with solvent. Indeed, the naked EP displayed very similar trends in hexane and toluene. Furthermore, Py-EP exhibited a significant viscosity drop when the solvent was switched from hexane to a hexane/toluene mixture containing 70 vol % of hexane. This behavior suggests that the polar associations taking place in hexane between the succinimide moieties are accountable for the formation of intra- (at low polymer concentrations) and inter- (at high polymer concentrations) molecular polymeric aggregates and that toluene is efficient at melting the polar associations and at hindering the formation of the interchain polymeric aggregates. The results presented in this study should be of interest to scientists involved in research on oil-additives since these polymers are used in engine oils as dispersants and viscosity index improvers.

**Acknowledgment.** The authors thank DSM, Imperial Oil, and NSERC (Canada) for financial support. M.Z. and J.D. acknowledge very helpful discussions with Drs. K. E. Fyfe, C. J. May, A. Blahey and J. Gao (Imperial Oil). J.D. is thankful to the funding provided by CFI and OIT associated with his being awarded a Tier-2 Canada Research Chair.

**Supporting Information Available:** A figure showing excitation spectra of Py-EP in hexane and toluene, tables listing the decay times and preexponential factors obtained from the fit of the Py-EP fluorescence decays with a sum of exponentials, tables listing the parameters retrieved from the blob model analysis of the Py-EP fluorescence decays, and text giving the details about the calculation of the Hansen solubility parameters of methyl succinimide. This material is available free of charge via the Internet at <http://pubs.acs.org>.

## References and Notes

- (1) van Duin, M. *Rec. Res. Dev. Macromol.* **2003**, *7*, 1–28.
- (2) Heinen, W.; Rosemoller, C. H.; Wenzel, C. B.; de Groot, H. J. M.; Lugtenburg, J.; van Duin, M. *Macromolecules* **1996**, *29*, 1151–1157.
- (3) Németh, S.; Jao, T.-C.; Fendler, J. H. *J. Polym. Sci., Part B: Polym. Phys.* **1996**, *34*, 1723–1732.
- (4) Németh, S.; Jao, T.-C.; Fendler, J. H. *Macromolecules* **1994**, *27*, 5449–5456.
- (5) Vangani, V.; Duhamel, J.; Németh, S.; Jao, T.-C. *Macromolecules* **1999**, *32*, 2845–2854.
- (6) Vangani, V.; Drage, J.; Mehta, J.; Mathew, A. K.; Duhamel, J. *J. Phys. Chem. B* **2001**, *105*, 4827–4839.
- (7) Zhang, M.; Duhamel, J.; van Duin, M.; Meessen, P. *Macromolecules* **2004**, *37*, 1877–1890.
- (8) Rubin, I. D. *CHEMTECH* **1987**, *17*, 620–623.
- (9) Guttierrez, A.; Brownawell, D. W.; Ricardo, B.; Johnston, J. E. US Patent 4,632,769, 1986.
- (10) Papke, B. L.; Bartley, L. S.; Migdal, C. A. *Langmuir* **1991**, *7*, 2614–2619.
- (11) Matsunaga, A.; Yagi, M. *Anal. Chem.* **1978**, *50*, 753–756.
- (12) Disanzo, F. P.; Herron, S. P.; Chawla, B.; Holloway, D. *Anal. Chem.* **1993**, *65*, 3359–3362.



- (13) Demas, J. N. *Excited-State Lifetime Measurements*; Academic Press: New York, 1983.
- (14) Press, W. H.; Flannery, B. P.; Teukolsky, S. A.; Vetterling, W. T. *Numerical Recipes. The Art of Scientific Computing (Fortran Version)*; Cambridge University Press: Cambridge, U.K., 1992.
- (15) Mathew, A. K.; Siu, H.; Duhamel, J. *Macromolecules* **1999**, *32*, 7100–7108.
- (16) Tachiya, M. *Chem. Phys. Lett.* **1975**, *33*, 289–292.
- (17) Infelta, P. P.; Gratzel, M.; Thomas, J. K. *J. Phys. Chem.* **1974**, *78*, 190–195.
- (18) Mathew, A. K.; Duhamel, J.; Gao, J. *Macromolecules* **2001**, *34*, 1454–1469.
- (19) Winnik, F. M. *Chem. Rev.* **1993**, *93*, 587–614.
- (20) Zhang, M.; Duhamel, J. Submitted to *Langmuir*.
- (21) Winnik, F. M.; Regismond, S. T. A. *Colloids Surf. A: Physicochem. Eng. Asp.* **1996**, *118*, 1–39.
- (22) Mizusaki, M.; Morishima, Y.; Yoshida, K.; Dubin, P. L. *Langmuir* **1997**, *13*, 6941–6946.
- (23) (a) Anghel, D. F.; Alderson, V.; Winnik, F. M.; Mizusaki, M.; Morishima, Y. *Polymer* **1998**, *39*, 3035–3044. (b) Hashidzume, A.; Mizusaki, M.; Yoda, K.; Morishima, Y. *Langmuir* **1999**, *15*, 4276–4282. (c) Suwa, M.; Hashidzume, A.; Morishima, Y.; Nakato, T.; Tomida, M. *Macromolecules* **2000**, *33*, 7884–7892.
- (24) Yamamoto, H.; Mizusaki, M.; Yoda, K.; Morishima, Y. *Macromolecules* **1998**, *31*, 3588–3594.
- (25) Yusa, S.-I.; Kamachi, M.; Morishima, Y. *Langmuir* **1998**, *14*, 6059–6067.
- (26) Nishikawa, K.; Yekta, A.; Pham, H. H.; Winnik, F. M.; Sau, A. C. *Langmuir* **1998**, *14*, 7119–7129.
- (27) Hecht, S.; Vladimirov, N.; Fréchet, J. M. J. *J. Am. Chem. Soc.* **2001**, *123*, 18–25.
- (28) Morishima, Y.; Nomura, S.; Ikeda, T.; Seki, M.; Kamachi, M. *Macromolecules* **1995**, *28*, 2874–2881.
- (29) Wang, C.; Tong, Z.; Zeng, F.; Ren, B.; Liu, X.; Wu, S. *Prog. Colloid Polym. Sci.* **2003**, *122*, 1–7.
- (30) de Melo, J. S.; Costa, T.; Miguel, M. D.; Lindman, B.; Schillén, K. *J. Phys. Chem. B* **2003**, *107*, 12605–12621.
- (31) Anghel, D. F.; Toca-Herrera, J. L.; Winnik, F. M.; Rettig, W.; von Klitzing, R. *Langmuir* **2002**, *18*, 5600–5606.
- (32) Nichifor, M.; Lopes, S.; Bastos, M.; Lopes, A. *J. Phys. Chem. B* **2004**, *108*, 16463–16472.
- (33) Lakowicz, J. R. *Principles of Fluorescence Spectroscopy*; Kluwer Academic/Plenum Publishers: New York, 1999.
- (34) Stryer, L.; Haugland, R. P. *Proc. Natl. Acad. Sci. U.S.A.* **1967**, *58*, 719–726.
- (35) Morawetz, H. *Science* **1988**, *240*, 172–176.
- (36) Mikes, F.; Morawetz, H.; Dennis, K. S. *Macromolecules* **1984**, *17*, 60–63.
- (37) (a) Mazuel, F.; Bui, C.; Charleux, B.; Cabet-Deliry, E.; Winnik, M. A. *Macromolecules* **2004**, *37*, 6141–6152. (b) Rharbi, Y.; Yekta, A.; Winnik, M. A.; DeVoe, R. J.; Barrera, D. *Macromolecules* **1999**, *32*, 3241–3248. (c) Duhamel, J.; Yekta, A.; Ni, S.; Khaykin, Y.; Winnik, M. A. *Macromolecules* **1993**, *26*, 7024–7030.
- (38) (a) Matejicek, P.; Uhlik, F.; Limpouchova, Z.; Prochazka, K.; Tuzar, Z.; Webber, S. E. *Macromolecules* **2002**, *35*, 9487–9496. (b) Uhlik, F.; Limpouchova, Z.; Matejicek, P.; Prochazka, K.; Tuzar, Z.; Webber, S. E. *Macromolecules* **2003**, *35*, 9497–9505.
- (39) Kujawa, P.; Liu, R. C. W.; Winnik, F. M. *J. Phys. Chem. B* **2002**, *106*, 5578–5585.
- (40) Yusa, S.-I.; Sakakibara, A.; Yamamoto, T.; Morishima, Y. *Macromolecules* **2002**, *35*, 10182–10188.
- (41) Mizusaki, M.; Morishima, Y.; Winnik, F. M. *Macromolecules* **1999**, *32*, 4317–4326.
- (42) (a) Smith, G. L.; McCormick, C. L. *Macromolecules* **2001**, *34*, 5579–5586. (b) Smith, G. L.; McCormick, C. L. *Macromolecules* **2001**, *34*, 918–924.
- (43) Duhamel, J.; Kanagalingam, S.; O'Brien, T.; Ingratta, M. *J. Am. Chem. Soc.* **2003**, *125*, 12810–12822.
- (44) Kanagalingam, S.; Ngan, C. F.; Duhamel, J. *Macromolecules* **2002**, *35*, 8560–8570.
- (45) Prazeres, T. J. V.; Beingessner, R.; Duhamel, J.; Olesen, K.; Shay, G.; Bassett, D. R. *Macromolecules* **2001**, *34*, 7876–7884.
- (46) Siu, H.; Duhamel, J. *Macromolecules* **2004**, *37*, 9287–9289.
- (47) Kanagalingam, S.; Spartalis, J.; Cao, T.-M.; Duhamel, J. *Macromolecules* **2002**, *35*, 8571–8577.
- (48) (a) Picarra, S.; Relogio, P.; Afonso, C. A. M.; Martinho, J. M. G.; Farinha, J. P. S. *Macromolecules* **2004**, *37*, 1670. (b) Picarra, S.; Relogio, P.; Afonso, C. A. M.; Martinho, J. M. G.; Farinha, J. P. S. *Macromolecules* **2003**, *36*, 8119–8129.
- (49) Picarra, S.; Duhamel, J.; Fedorov, A.; Martinho, J. M. G. *J. Phys. Chem. B* **2004**, *108*, 12009–12015.
- (50) Jansens, L. D.; Boens, N.; Ameloot, M.; De Schryver, F. C. J. *Phys. Chem.* **1990**, *94*, 3564–3576.
- (51) Gehlen, M. H.; De Schryver, F. C. *Chem. Rev.* **1993**, *93*, 199–221.
- (52) Bandrup, J.; Immergut, E. H.; Grulke, E. A. *Polymer Handbook*, 4th ed.; John Wiley & Sons: New York, 1999; p VII 675–683.
- (53) Barton, A. F. M. *Chem. Rev.* **1975**, *75*, 731–753.

MA0505528